IFJPAN-V-2005-07
hep-ph/0703043

SANCnews: Sector $4f$, Charged Current

A. Arbuzov[1,2], D. Bardin[2], S. Bondarenko[1,2], P. Christova[2], L. Kalinovskaya[2], G. Nanava[3], R. Sadykov[2], W. von Schlippe[4]

[1] *Bogoliubov Laboratory of Theoretical Physics, JINR, Dubna, RU-141980, Russia*
[2] *Dzhelepov Laboratory of Nuclear Problems, JINR, Dubna, RU-141980, Russia*
[3] *IFJ, PAN, Krakow, Poland*
[4] *PNPI, St. Petersburg, RU-188300, Russia*

Abstract

In this paper we describe the implementation of the charged current decays of the kind $t \to bl^+\nu_l(\gamma)$ into framework of `SANC` system. All calculations are done taking into account one-loop electroweak correction in the Standard Model. The emphasis of this paper is done on the presentation of numerical results. Various distributions are produced by means of a Monte Carlo integrator and event generator. Comparison with the results of CompHEP and PYTHIA packages are presented for the Born and hard photon contributions. The validity of the cascade approximation at one-loop level is also studied.

Submitted to EPJC

This work is partly supported by INTAS grant N^o 03-51-4007
and by the EU grant mTkd-CT-2004-510126 in partnership with the CERN Physics Department and by the Polish Ministry of Scientific Research and Information Technology grant No 620/E-77/6.PRUE/DIE 188/2005-2008.

1 Introduction

In this paper we describe a further application of the computer system SANC *Support of Analytic and Numerical calculations for experiments at Colliders* intended for semi-automatic calculations of realistic and pseudo-observables for various processes of elementary particle interactions at the one-loop precision level (see Ref.[1] and references therein).

Here we concentrate on the implementation of the 4 legs decay $t \to b + l^+ + \nu_l$ as a typical example of the charged current (CC) decay of the kind $F \to f + f_1 + \bar{f}_1'$ where F and f stand for massive fermions and f_1 and $\bar{f}_1'$ for massless fermions. In this paper we continue to present the physical applications of the SANC system, started in Ref.[2] rather than present extension of the system itself as continued in Ref.[3].

According to the SM the dominant channel of top quark decay is $t \to bW^+$ with a branching ratio of 99.9%. The decay branching ratio of the W boson into leptons is $\mathrm{Br}(W \to l^+\nu_l) \approx 11\%$ Ref.[4]. Therefore, the semileptonic decays $t \to bl^+\nu_l$ ($l^+ \equiv e^+$, μ^+, τ^+) amount to approximately 1/3 of all top quark decays.

This paper is devoted to the complete one-loop QED and EW radiative corrections (EWRC) to the 4 legs semileptonic top quark decay $t \to bl^+\nu_l(\gamma)$. The calculation of QCD corrections in SANC for these 3 and 4 legs top decays is presented in Ref.[5].

EW and QCD radiative corrections to the 3 legs decay $t \to bW^+$ were first calculated in the papers[6, 7, 8] and relevant issues may be found in Refs.[9, 10, 11, 12, 13, 14, 15]; even two-loop QCD corrections are known [16, 17, 18]. However, we are not aware of papers where the 4 legs top decay $t \to bl^+\nu_l$ would be considered at one-loop.

The results for the Born level decay width, presented in this paper, are compared with the calculation performed by means of CompHEP [19] and PYTHIA [20] packages and those for the 5 legs accompanying bremsstrahlung — with the results of CompHEP. We also discuss briefly how our results for the one-loop EW corrections are compared with results existing in the literature. The validity of the cascade approximation is also studied.

The paper is organized as follows. In section 2 we briefly recall the calculational scheme adopted in SANC . The Born level is given in section 3 and the one-loop EW corrections in section 4. Various numerical results are collected in section 5. In section 6 we discuss the cascade approach to the problem, and in section 7 we present some conclusions. We assume that the reader may run SANC as described in section 6 of Ref.[1] in order to see all relevant formulae which are not presented in this paper and get the corresponding numbers.

2 Calculation scheme

Recall that SANC performs calculations starting from the construction of EW form factors (FF) which parameterize the covariant amplitude (CA) and helicity amplitudes (HA) of a process. From HA, the s2n software produces the FORTRAN codes for them and then the differential decay width is computed numecally. These codes can be further used in MC generators and integrators. The amplitudes (CA and HA) for the 4 legs top and

antitop decays are presented in Ref.[1].

These two ingredients, together with accompanying bremsstrahlung (BR) are accessible via menu sequence **SANC → EW → Processes → 4 legs → 4f → Charged current → t −> b l nu → t −> b l nu (FF, HA, BR)**, see Fig.1. A FORM (see Ref.[21]) module, loaded at the end of this chain computes on-line the FF, HA and BR, respectively. For more detail see section 2.5 of the `SANC` description in Ref.[1] and the book[22].

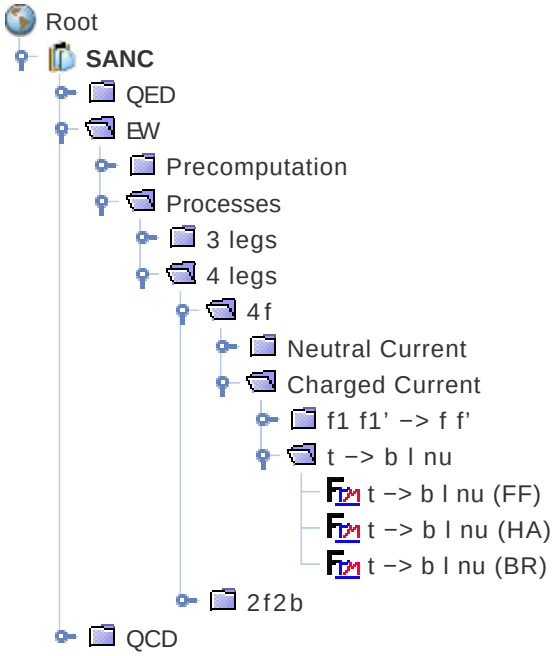

Figure 1: `SANC` tree for $t \to bl^+\nu_l$ decay.

The total one-loop width, $\Gamma^{1-\mathrm{loop}}$, of the decay $t \to bl^+\nu_l(\gamma)$ can be subdivided into the following terms:

$$\begin{aligned} \Gamma^{1-\mathrm{loop}} &= \Gamma^{\mathrm{Born}} + \Gamma^{\mathrm{virt}}(\lambda) + \Gamma^{\mathrm{real}}(\lambda,\bar{\omega}), \\ \Gamma^{\mathrm{real}}(\lambda,\bar{\omega}) &= \Gamma^{\mathrm{soft}}(\lambda,\bar{\omega}) + \Gamma^{\mathrm{hard}}(\bar{\omega}). \end{aligned} \tag{1}$$

Here Γ^{Born} is the decay width in the Born approximation, Γ^{virt} is the virtual contribution, Γ^{soft} and Γ^{hard} are the contributions due to the soft and hard photon emission respectively. The auxiliary parameter $\bar{\omega}$ separates the soft and hard photon contributions and the parameter λ ("photon mass"), which enters the virtual and soft contributions, regularizes the infrared divergences.

We present numbers, collected for the standard `SANC INPUT`, PDG(2006) [23]:

$$\begin{array}{llllll} G_F = 1.16637\cdot 10^{-5}\,\mathrm{GeV}^{-2}, & \alpha(0) = 1/137.03599911 & & & & \\ M_W = 80.403\,\mathrm{GeV}, & \Gamma_W = 2.141\,\mathrm{GeV}, & & & & \\ M_Z = 91.1876\,\mathrm{GeV}, & \Gamma_Z = 2.4952\,\mathrm{GeV}, & & & & \\ M_H = 120\,\mathrm{GeV}, & & & & & \\ m_e = 0.51099892\cdot 10^{-3}\,\mathrm{GeV}, & m_u = 62\,\mathrm{MeV} & & & m_d = 83\,\mathrm{MeV}, & \\ m_\mu = 0.105658369\,\mathrm{GeV}, & m_c = 1.5\,\mathrm{GeV}, & & & m_s = 215\,\mathrm{MeV}, & \\ m_\tau = 1.77699\,\mathrm{GeV}, & m_b = 4.7\,\mathrm{GeV}, & & & m_t = 174.2\,\mathrm{GeV}. & \end{array}$$

The coupling constants can be set to different values according to the different input parameter schemes. They can be directly identified with the fine-structure constant $\alpha(0)$ together with $e/g = s_W$ and $c_W = M_W/M_Z$. This choice is called α scheme. Another one, the G_F scheme, makes use of the Fermi constant and the quantity Δr. Note, we do not iterate the equation for Δr. We use both schemes to produce numbers.

3 Born-level process

In the Born approximation there is only one Feynman diagram for the decay $t \to bl^+\nu_l$ with one intermediate virtual W^+ boson, see Fig.2.

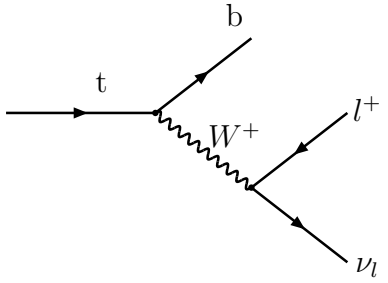

Figure 2: Feynman diagram for Born level process.

The differential decay rate reads:

$$d\Gamma^{\rm Born} = \frac{1}{2m_t}\overline{\sum_{spins}}|\mathcal{M}^{\rm Born}|^2 d\Phi^{(3)}\,, \tag{2}$$

where $\mathcal{M}^{\rm Born}$ is the amplitude of the process and $d\Phi^{(3)}$ is the differential three-body phase space:

$$d\Phi^{(3)} = \Phi_1^{(2)}\, d\Phi_2^{(2)}\, \frac{ds}{2\pi}\,, \tag{3}$$

expressed in terms of the two-body phase spaces:

$$\begin{aligned} \Phi_1^{(2)} &= \frac{1}{8\pi}\frac{\sqrt{\lambda(m_t^2, m_b^2, s)}}{m_t^2}\,, \\ d\Phi_2^{(2)} &= \frac{1}{8\pi}\frac{\sqrt{\lambda(s, m_l^2, 0)}}{s}\frac{1}{2} d\cos\theta\,. \end{aligned} \tag{4}$$

One can express the values $|\mathcal{M}^{\rm Born}|^2$ and $d\Phi^{(3)}$ via two independent variables: $s = -(p_l + p_\nu)^2$ and $\cos\theta$, where θ is the angle between $\vec{p_l}$ and $\vec{p_b}$ in the rest frame of the compound (l^+, ν_l). The limits of variation are:

$$m_l^2 \le s \le (m_t - m_b)^2\,, \qquad -1 \le \cos\theta \le +1\,. \tag{5}$$

If the lepton mass is not ignored, then the s and ϑ dependence of the Mandelstam variables t and u is given by

$$(t,u) = m_b^2 + m_l^2 + \frac{1}{2s}\Big[\left(s + m_l^2\right)\left(m_t^2 - m_b^2 - s\right) \mp \left(s - m_l^2\right)\sqrt{\lambda_s}\cos\theta\Big], \tag{6}$$

where $\lambda_s = (m_t^2 + m_b^2 - s)^2 - 4m_b^2 m_t^2$.

The result of the two-fold Monte Carlo integration is shown in Table 1. This calculation is performed by means of a Monte Carlo integration routine based on the VEGAS algorithm Ref.[24]. The numbers produced with help of CompHEP and PYTHIA packages are also presented in the table. The results of SANC and CompHEP are in a good

$\Gamma^{\rm Born}$, GeV		
SANC	CompHEP	PYTHIA
0.16936(1)	0.16935(1)	0.16782(1)

Table 1: Born-level decay width for decay $t \to b\mu^+\nu_\mu$ produced by SANC , CompHEP and PYTHIA.

agreement, the deviation from PYTHIA appears due to the difference in the definition of EW constants. In addition to integration we use a Monte Carlo generator of unweighted events to produce differential distributions. In Fig.3 we present some of these distributions and a comparison with distributions, obtained with help of CompHEP and PYTHIA packages. We note, that the input parameters for this comparison were tuned to CompHEP. In Figures 3–4 we show a triple comparison for the four distributions over various kinematical variables at the Born level.

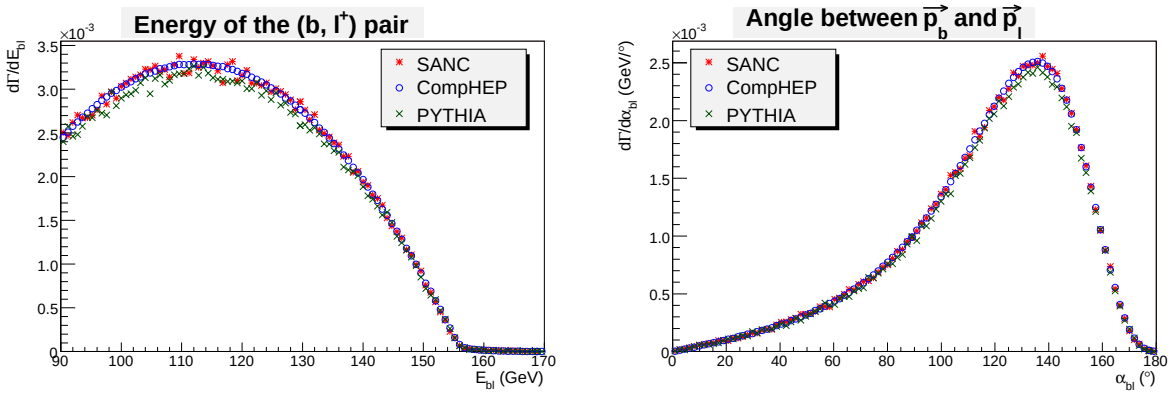

Figure 3: Differential distributions for process $t \to b\mu^+\nu_\mu$ of the $b\mu^+$ pair energy and the angle between $\vec{p}_b$ and $\vec{p}_l$ produced with help of SANC , CompHEP and PYTHIA.

The figures demonstrate a very good agreement between SANC and CompHEP and a fair agreement with PYTHIA.

4 Radiative corrections

Radiative corrections can be subdivided into two parts: *virtual (one-loop)* corrections and *real (single photon emission)*. The latter, in turn, is subdivided into *soft* and *hard* photon emission, see Eq. (1).

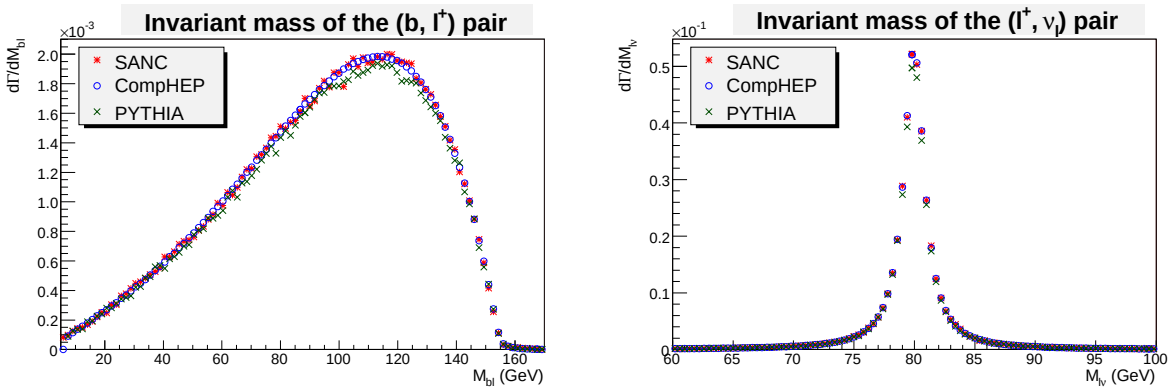

Figure 4: Differential distributions for process $t \to b\mu^+\nu_\mu$ of invariant masses of $b\mu^+$ and $\mu^+\nu_\mu$ pairs produced by `SANC` , CompHEP and PYTHIA.

4.1 Virtual corrections

Virtual corrections can be schematically represented by building block diagrams: dressed vertices, self-energies and boxes, see Fig.5. They all, except the boxes, include relevant counterterm contributions in the same spirit as described for the neutral current (NC) case in Ref.[25]. We also apply the recipe of Ref.[26] to regularize the so-called "on-mass-shell" singularities.

The virtual contribution is parameterized by scalar form factors which can be found in the "`SANC Output window`" after a run of the FF-module on the top decay branch of the `SANC` tree, see Fig.1.

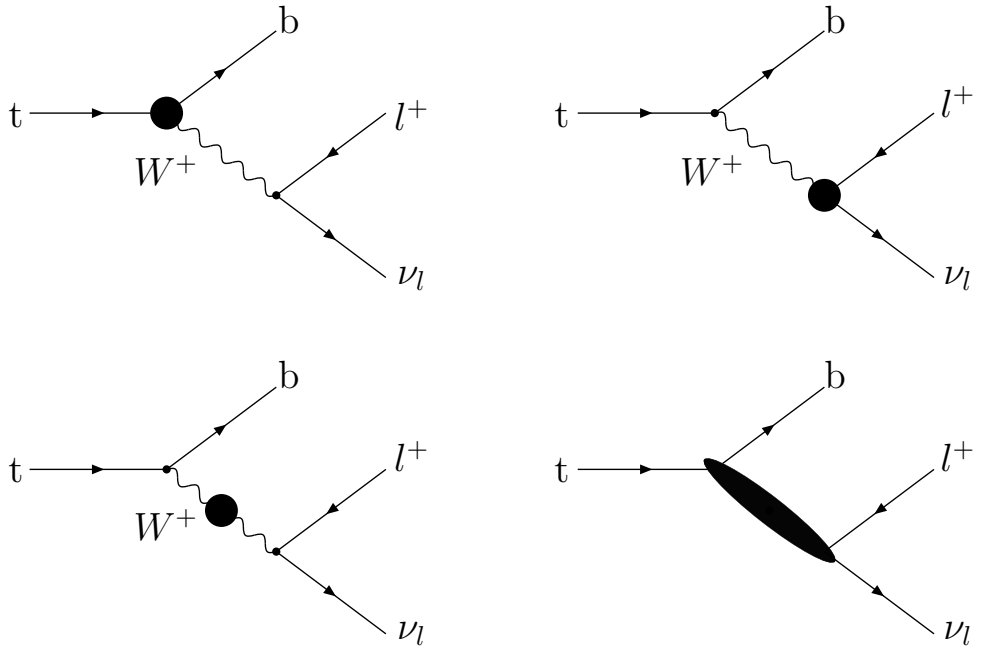

Figure 5: Feynman diagrams for one-loop level decay.

4.2 Real corrections

The soft contribution is proportional to the Born level decay rate and has the same phase space. Its explicit expression can also be found in the "`SANC Output window`" after `SANC` -run of BR-module, see Fig.1.

For hard photon emission there are four tree-level Feynman diagrams (see Fig.6). One diagram corresponds to emission from the initial state, two diagrams describe the final state radiation and the remaining diagram corresponds to radiation from the intermediate W^+ boson.

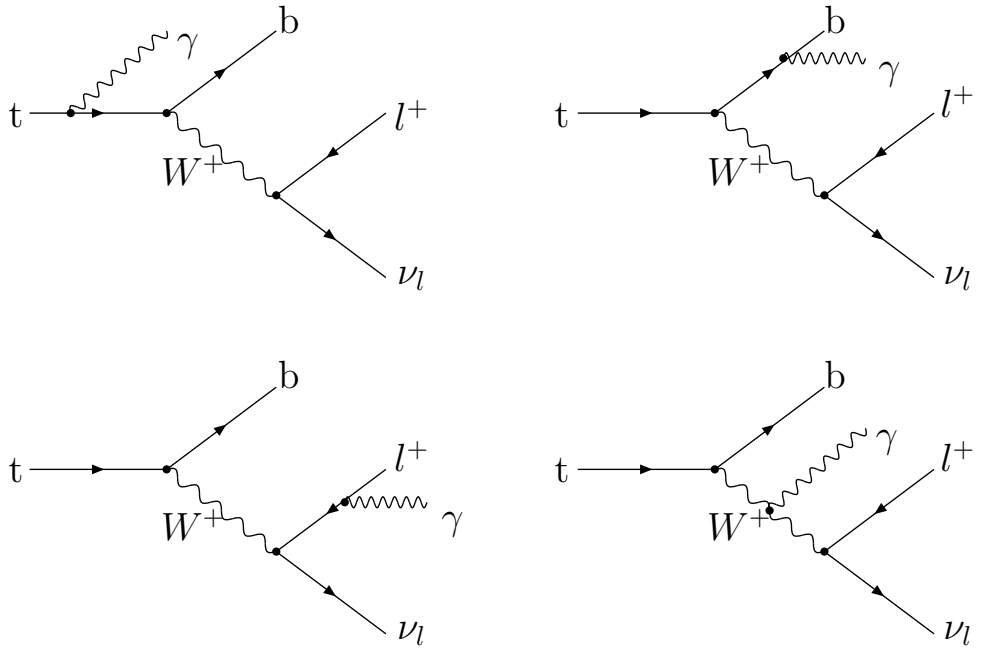

Figure 6: Feynman diagrams for hard photon emission.

Hard bremsstrahlung in $t(p_1) \to b(p_2) + l^+(p_3) + \nu_l(p_4) + \gamma(p_5)$ has the four-body phase space:

$$d\Phi^{(4)} = \Phi_1^{(2)} d\Phi_2^{(2)} d\Phi_3^{(2)} \frac{ds_{25}}{2\pi} \frac{ds_{34}}{2\pi}\,, \tag{7}$$

where the three two-body phase spaces are:

$$\begin{aligned}
\Phi_1^{(2)} &= \frac{1}{8\pi} \frac{\sqrt{\lambda(m_t^2, s_{25}, s_{34})}}{m_t^2}\,, \\
d\Phi_2^{(2)} &= \frac{1}{8\pi} \frac{\sqrt{\lambda(s_{25}, m_b^2, 0)}}{s_{25}} \frac{1}{2} d\cos\theta_1\,, \\
d\Phi_3^{(2)} &= \frac{1}{8\pi} \frac{\sqrt{\lambda(s_{34}, m_l^2, 0)}}{s_{34}} \frac{1}{2} d\cos\theta_2 d\phi_2\,.
\end{aligned} \tag{8}$$

The kinematics and meaning of variables are illustrated in Fig.7.

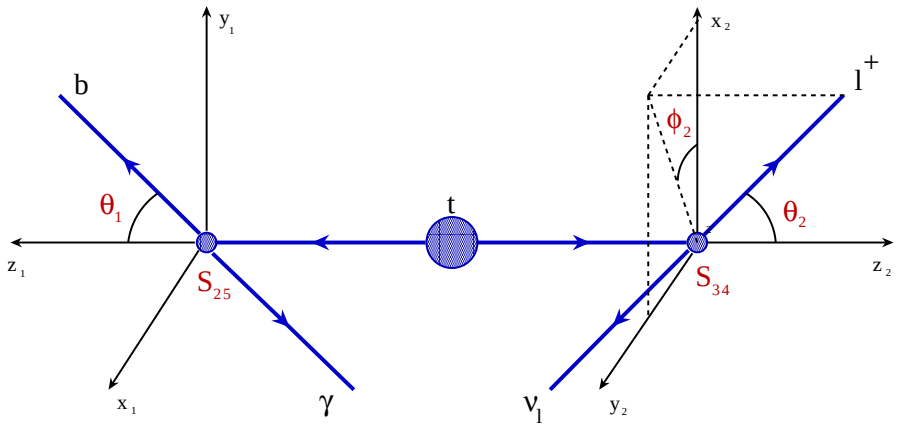

Figure 7: Kinematical diagram for hard photon emission.

The total decay rate for the hard process is represented by a 5-fold integral over s_{25}, s_{34}, $\cos\theta_1$, $\cos\theta_2$, ϕ_2, varying within the following limits:

$$\begin{aligned} m_b^2 \le s_{25} \le (m_t - m_l)^2, \\ m_l^2 \le s_{34} \le (m_t - \sqrt{s_{25}})^2, \\ -1 \le \cos\theta_1 \le +1\,, \\ -1 \le \cos\theta_2 \le +1\,, \\ 0 \le \phi_2 \le 2\pi\,. \end{aligned} \tag{9}$$

The matrix element of Fig.6 and the kinematics described in this section are basis for the SANC Monte Carlo generator.

5 Numerical results

5.1 Comparison of hard bremsstrahlung between SANC and CompHEP.

We begin by presenting the results of the Monte Carlo integration of the hard photon contributions derived with the help of SANC and CompHEP as presented in Table 2.

There is a significant difference between two sets of numbers and this difference increases with decreasing $\bar{\omega}$. This difference is due to the approximate representation of the W boson propagators implemented in CompHEP; in CompHEP the complex propagator is used in a real representation:[1]

$$\frac{1}{p^2 - M_W^2 + iM_W\Gamma_W} \to \frac{p^2 - M_W^2}{(p^2 - M_W^2)^2 + M_W^2\Gamma_W^2}\,. \tag{10}$$

[1]Here we use exceptionally the metric $p^2 = M^2$.

$\bar{\omega}$, GeV	$\Gamma^{\rm hard}$, 10^{-2}GeV CompHEP	$\Gamma^{\rm hard}$, 10^{-2}GeV SANC
10	0.2578(2)	0.2592(2)
1	0.6982(3)	0.8582(2)
10^{-1}	0.8538(3)	1.5000(3)
10^{-2}	0.9628(4)	2.1495(3)
10^{-3}	1.0730(4)	2.8005(4)
10^{-4}	1.1809(3)	3.4525(4)

Table 2: Comparison for hard emission produced by SANC and CompHEP systems for $E_\gamma \geq \bar{\omega}$.

This assumption will not lead to a noticeable departure from the correct result with the exception of the case when we have the product of two different W propagators (i.e. with different virtualities). In this case it is necessary to make a substitution that corrects this assumption:

$$\frac{p_1^2-M_W^2}{(p_1^2-M_W^2)^2+M_W^2\Gamma_W^2}\,\frac{p_2^2-M_W^2}{(p_2^2-M_W^2)^2+M_W^2\Gamma_W^2} \rightarrow \frac{p_1^2-M_W^2}{(p_1^2-M_W^2)^2+M_W^2\Gamma_W^2}\,\frac{p_2^2-M_W^2}{(p_2^2-M_W^2)^2+M_W^2\Gamma_W^2} + \frac{M_m^2\Gamma_W^2}{((p_1^2-M_W^2)^2+M_W^2\Gamma_W^2)((p_2^2-M_W^2)^2+M_W^2\Gamma_W^2)}\,. \tag{11}$$

We can explicitly observe the difference in Fig.8, where we present the various differential distributions. As indicated in the upper two pictures the difference is to be seen in the region of soft photon emission near the resonance.

Note, that if we use recipe (10) in SANC , then we simulate the CompHEP distributions with a very good precision.

5.2 Numerical results for the complete EWRC

The results for the complete one-loop calculation of widths in α and G_F schemes and comparison with Born level widths are presented in the Tables 3 and 4.[2]

l	$\Gamma^{\rm Born}$, GeV	$\Gamma^{\rm 1-loop}$, GeV	δ, %
l^+	0.14948(1)	0.16064(1)	7.47

Table 3: Born and one-loop decay width and percentage of the correction in α scheme.

[2]NB: Although SANC may produce all results exact in b-mass, all numbers in this subsection and section 6 are derived for $m_b \to 0$.

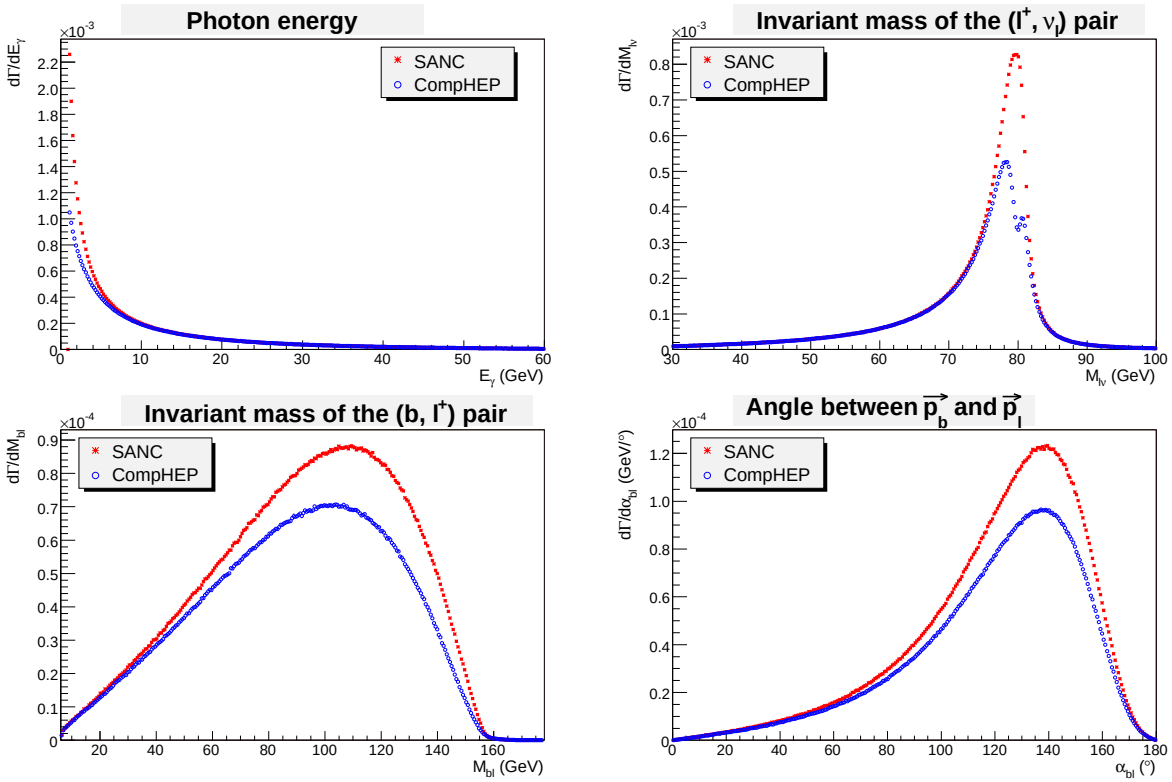

Figure 8: Differential distributions for hard photon emission process $t \to b\mu^+\nu_l\gamma$ with $E_\gamma \geq 1$ GeV.

l	$\Gamma^{\rm Born}$, GeV	$\Gamma^{\rm 1-loop}$, GeV	δ, %
l^+	0.16018(1)	0.16299(1)	1.75

Table 4: Born and one-loop decay width and percentage of the correction in G_F scheme.

There is practically no sensitivity to the lepton mass since it is neglected everywhere but in arguments of logs which, in turn, are vanishing due to the KLN theorem.

6 EWRC in cascade approximation

It is interesting to compare results of the complete approach with an approximate, "cascade" calculation based on the formula (we consider the case $l = e$):

$$\Gamma_{t\to be\nu} = \frac{\Gamma_{t\to Wb}\Gamma_{W\to e\nu}}{\Gamma_W}\,. \tag{12}$$

The input parameters are as in Eq. (2), except m_b which is set to zero here, and we present results in the α and G_F schemes. Consider first the validity of Eq. (12) at the Born level for a (*formal*) variation of Γ_W, see Table 5:

	$\Gamma^{\rm Born}$, GeV	$\Gamma^{\rm Born}_{\rm cascade}$, GeV	$\delta, \%$
Γ_W	0.14948	0.15187	1.6
$\Gamma_W/10$	1.5163	1.5187	0.2
$\Gamma_W/10^2$	15.185	15.187	0.01
$\Gamma_W/10^3$	151.87	151.87	0.00

Table 5: Comparison of Born widths without and with cascade approximation, $\alpha(0)$-scheme.

The cascade approximation at the Born level improves rapidly with decreasing Γ_W. Complete one-loop calculations are shown in Tables 6–7.

	$\Gamma^{\rm Born}$, GeV	$\Gamma^{\rm 1-loop}$, GeV	$\delta, \%$
Γ_W	0.14949	0.16064	7.46

Table 6: Born and one-loop decay width and percentage of the correction, $\alpha(0)$-scheme.

	$\Gamma^{\rm Born}$, GeV	$\Gamma^{\rm 1-loop}$, GeV	$\delta, \%$
Γ_W	0.16018	0.16299	1.75

Table 7: Born and one-loop decay width and percentage of the correction, G_F-scheme.

Now turn to the one-loop version of cascade Eq. (12). First, compute $\Gamma(t \to Wb)$ and $\Gamma(W \to e\nu)$ neglecting Γ_W in all W boson propagators (10). So, in Eq. (12) the numerator does not depend on Γ_W. In this "naive" variant of calculations it is sufficient to consider only one point over Γ_W, since the correction δ is a constant by construction.

	$t \to Wb$	$W \to e\nu$	$t \to be\nu$ cascade
$\Gamma^{\rm Born}$, GeV	1.4800	0.21970	0.15187
$\Gamma^{\rm 1-loop}$, GeV	1.5466	0.22528	0.16274
$\delta, \%$	4.49	2.54	7.15

Table 8: Born, one-loop decay widths and percentage of the correction in cascade approximation, $\alpha(0)$-scheme.

From Tables 6–9 one sees that the complete and cascade one-loop calculations deviate considerably. This hints to take into account effects of Γ_W in cascade calculations more carefully.

At the end of this section we note that the percentage of EWRC correction for $t \to Wb$ decay reasonably agrees with results given in Table 1 of Ref.[6], even though we did not tune any parameters to achieve agreement.

	$t \to Wb$	$W \to e\nu$	$t \to be\nu$ cascade
$\Gamma^{\rm Born}$, GeV	1.5321	0.22742	0.16274
$\Gamma^{\rm 1-loop}$, GeV	1.5572	0.22670	0.16488
δ, %	1.64	-0.32	1.31

Table 9: Born, one-loop decay widths and percentage of the correction in cascade approximation, G_F-scheme.

7 Conclusions

A study of the semileptonic top quark decay $t \to bl^+\nu_l(\gamma)$ was presented. We have computed the total one-loop electroweak corrections to this process with the aid of the `SANC` system. Using a Monte Carlo integrator and an event generator that we have created for this purpose, we specify the influence on the decay width due to EWRC. These corrections are about 7.5% for α scheme and approximately 1.8% for G_F scheme. The comparison with the numbers of CompHEP and PYTHIA packages was done at the tree level. During this comparison we found noticeable deviation from the CompHEP package for soft photon emission in the resonance region.

We have studied the cascade approach to the problem under consideration. We have shown that the "naive" approach with "stable" W's is not precise enough. An improved treatment of the cascade approach with the complex W mass will be presented elsewhere.

Acknowledgments

This work was partly supported by the INTAS grant 03-41-1007 (AA, DB, SB and LK) by the RFBR grant 04-02-17192 (AA) and by the EU grant mTkd-CT-2004-510126 in partnership with the CERN Physics Department and by the Polish Ministry of Scientific Research and Information Technology grant No 620/E-77/6.PRUE/DIE 188/2005-2008 (GN). AA, DB, SB, LK and GN are indebted to the directorate of IFJ, Krakow, for hospitality which was extended to them in April–May 2005, when an essential part of this study was done.

References

[1] A. Andonov *et al.*, Comput. Phys. Commun. **174** (2006) 481–517.

[2] A. Arbuzov *et al.*, Eur. Phys. J. C **46** (2006) 407.

[3] D. Bardin, S. Bondarenko, L. Kalinovskaya, G. Nanava, L. Rumyantsev and W. von Schlippe, "SANCnews: Sector $ffbb$," hep-ph/0506120.

[4] *ATLAS detector and physics performance Technical Design report*, Volume II, 1999.

[5] A. Andonov, A. Arbuzov, S. Bondarenko, P. Christova, V. Kolesnikov and R. Sadykov, *QCD branch in SANC*, Pisma v ECHAYA, N6 (2007).

[6] A. Denner and T. Sack, Nucl. Phys. B **358** (1991) 46.

[7] G. Eilam, R. R. Mendel, R. Migneron and A. Soni, Phys. Rev. Lett. **66** (1991) 3105.

[8] B. A. Irwin, B. Margolis and H. D. Trottier, Phys. Lett. B **256** (1991) 533.

[9] T. Kuruma, Z. Phys. C **57** (1993) 551.

[10] B. Lampe, Nucl. Phys. B **454** (1995) 506.

[11] S. M. Oliveira, L. Brucher, R. Santos and A. Barroso, Phys. Rev. D **64** (2001) 017301.

[12] M. Fischer, S. Groote, J. G. Korner and M. C. Mauser, Phys. Rev. D **65** (2002) 054036.

[13] H. S. Do, S. Groote, J. G. Korner and M. C. Mauser, Phys. Rev. D **67** (2003) 091501.

[14] B. H. Smith and M. B. Voloshin, Phys. Lett. B **340** (1994) 176.

[15] S. Mrenna and C. P. Yuan, Phys. Rev. D **46** (1992) 1007.

[16] K. G. Chetyrkin, R. Harlander, T. Seidensticker and M. Steinhauser, [arXiv:hep-ph/9910339].

[17] M. Slysarczyc, *Two-loop QCD corrections to top quark decay*, Lake Louise 2004, Fundamental interactions, 284-288, [arXiv:hep-ph/0401026].

[18] Q. H. Cao and C. P. Yuan, Phys. Rev. Lett. **93** (2004) 042001.

[19] E. Boos *et al.* [CompHEP Collaboration], Nucl. Instrum. Meth. A **534** (2004) 250.

[20] T. Sjostrand, S. Mrenna and P. Skands, JHEP **0605** (2006) 026.

[21] J. A. M. Vermaseren, *New features of FORM*, `math-ph/0010025`.

[22] D. Bardin, G. Passarino, *The Standard Model in the Making: Precision Study of Electroweak Interactions*, Oxford, Clarendon, 1999.

[23] URL: *http://pdg.lbl.gov/2006/tables/contents_tables.html*.

[24] G. P. Lepage, J. Comput. Phys. **27** (1978) 192.

[25] A. Andonov *et al.*, Phys. Part. Nucl. **34** (2003) 577; [Fiz. Elem. Chast. Atom. Yadra **34** (2003) 1125].

[26] D. Wackeroth and W. Hollik, Phys. Rev. D **55** (1997) 6788.